

A fast avalanche Si diode with a 517 μm low-doped region

Cite as: Appl. Phys. Lett. **117**, 013501 (2020); doi: 10.1063/5.0016228

Submitted: 3 June 2020 · Accepted: 22 June 2020 ·

Published Online: 6 July 2020







View Online



Export Citation



CrossMark

Amit S. Kesar,^{1,a)}  Arie Raizman,¹ Gil Atar,¹ Shoval Zoran,¹  Svetlana Gleizer,² Yakov Krasik,² 
and Doron Cohen-Elias¹ 

AFFILIATIONS

¹Department of Applied Physics, Soreq NRC, Yavne 81800, Israel

²Department of Physics, Technion, Haifa 32000, Israel

^{a)} Author to whom correspondence should be addressed: kesar@soreq.gov.il

ABSTRACT

A silicon-avalanche shaper/sharpener is a fast-closing semiconductor switch. For positive voltages, it is activated by a high-voltage pulse at its cathode, and, when turned on, the current through the device rises rapidly. Using Synopsys TCAD software, a $p^+ - n - n^+$ diode is numerically studied. It was shown that for the case of a high-doped active n region, 10^{14} cm^{-3} , the breakdown process exhibits a fast electric field propagation, as expected. For a low doped active n region, $< 10^{11} \text{ cm}^{-3}$, the electric field spreads uniformly along the structure. For this case, we show that the rise time, of the order of 100 ps, is not limited by the active region thickness, allowing the use of a thicker substrate in order to increase the operating voltage. A $p^+ - n - n^+$ diode was fabricated on a thick, 525 μm , float-zone n -type Si (100) substrate, with a resistivity of $10^4 \Omega \text{ cm}$. The active region, $n < 10^{12} \text{ cm}^{-3}$, was 517 μm . When a stack of five, 8 mm^2 , diodes was driven by an $\sim 100 \text{ kV}$, 2.26 ns rise time pulse, the output voltage was 46 kV with the rise time and rise rate per diode of 215 ps and 38.4 kV/ns, respectively. When a single, 4 mm^2 , diode was driven by a 14 kV, 1 ns rise time pulse, the output on a 50 Ω load was around 8 kV, 100 ps, with a rise rate of 57 kV/ns. These results exceed the present state-of-the-art diodes. Furthermore, the thick active region eliminates current fabrication process difficulties such as deep diffusion or thick epitaxial layers.

Published under license by AIP Publishing. <https://doi.org/10.1063/5.0016228>

Fast high-voltage diodes, such as a silicon-avalanche shaper (SAS), a semiconductor opening switch (SOS), and a drift-step-recovery diode (DSRD),^{1–13} can be used for various applications such as plasma discharge experiments¹⁴ and for ultra-wideband pulse generation.^{15,16} The SAS is a fast closing semiconductor switch.¹⁷ For the applied positive voltages, it operates in the negative, cathode to anode, direction. It receives a positive high-voltage pulse at its cathode, and when turned on, the current through the device rises rapidly. Typical input voltages are of the order of a few kilovolts, with a rise time of the order of 1 ns. The device turn-on time is of the order of 100 ps. A similar function is obtained with devices known as dynistors^{18–20} and delayed breakdown devices (DBDs).²¹

The diode's turn on occurs in two stages.²² At input voltage ramp up, the electric field across the diode increases. During this stage, the current passing through the diode is dominated by the displacement current, resulting in a pre-pulse at the output load. The second stage occurs at a dynamic breakdown voltage, which exceeds the stationary breakdown voltage. The electric field rises above a dynamic threshold,

$E_{\text{avalanche}}$ of some $\sim 300 \text{ kV/cm}$ for silicon. This results in an avalanche ionization process in the active region.

A typical silicon diode structure is $p^+ - n - n^+$, where n is the active region, having a thickness of 100–300 μm with a phosphorous doping of about 10^{14} cm^{-3} .^{16,22} It has been shown that in order to obtain fast, 100-ps scale pulses, the device active region, i.e., its n layer, has to be in the range of 100–200 μm .^{16,21–25} The two major disadvantages of using a thin active region are the limited breakdown voltage and fabrication process challenges such as deep diffusion into thin substrates or thick epitaxial layers.

In order to reduce this scaling requirement, one can use a low-doped substrate with a doping concentration $n < 10^{12} \text{ cm}^{-3}$,⁸ where in Ref. 8, simulations of uniform breakdown were presented for the first time for a 100 μm active region. With low doping, a SAS with an active region wider than 100 μm could be fully depleted with an almost-uniform electric field along the entire n layer. Thus, the avalanche process occurs simultaneously across the whole depletion region, and the switching rise time is not limited by the thickness of the n layer, but rather by the internal discharge time. This discharge time is explained in Ref. 8.

In addition, the breakdown voltage is maximized to $E_{avalanche} \times W$, and the junction capacitance $C_A = C/A = \epsilon_r \epsilon_0 / W$ and the displacement current $J_D = C_A \times dV_d/dt$ in the pre-pulse region decrease compared to a thin n -layer case. Here, W is the depletion region width, ϵ_r and ϵ_0 are the relative and vacuum permittivities, respectively, A is the junction area, and V_d is the voltage drop on the SAS diode.

In this study, we simulated and fabricated SAS diodes with a low-doped n layer. Finally, a stack of five thick diodes, based on a 525 μm substrate with a resistivity of $10^4 \Omega \text{ cm}$, was fabricated, diced, and connected in series. A peak load voltage of 46 kV was measured, with a maximum rise rate at the load of 192 kV/ns. The output rise time was 215 ps. With a single diode, an 8 kV pulse with a rise time and rise rate of 100 ps and 57 kV/ns was obtained, respectively.

Synopsys TCAD software was used to simulate the SAS diodes.^{26,27} The Van Overstraeten-de Man Model, based on the Chynoweth law,²⁸ was used for avalanche generation of the electron-hole pairs with the quasi-Fermi level gradient, $F_{ava} = |\nabla \Phi_{n,p}|$, as the driving force for impact ionization. We note that the same results were obtained with or without activating the Band-to-Band Tunneling Simple Model.²⁹ The latter allows us to consider the avalanching model for explanations of the results obtained in the present research.

Two $p^+ - n - n^+$ diodes, with the n region having a thickness of 100 μm and a junction area of 4 mm^2 , were simulated, one with $n = 1.5 \times 10^{10} \text{ cm}^{-3}$ and the other with $n = 10^{14} \text{ cm}^{-3}$. We note that the low-doped value, $1.5 \times 10^{10} \text{ cm}^{-3}$, represents a doping level, which is around the intrinsic concentration in silicon. Simulation results were practically the same for any doping levels below 10^{11} cm^{-3} . The static breakdown voltages for the low- and high-doped diodes were 1.65 kV and 1.31 kV, respectively.

The input voltage was a half-sine of 2 ns and an amplitude of 3 kV. The diode was connected in series between the input voltage source and the load, $R_{Load} = 50 \Omega$. Figure 1 shows the simulation results vs time. The voltage on the diodes is shown in Fig. 1(a). The peak of the diode voltage was 2.53 kV and 2.14 kV for the $1.5 \times 10^{10} \text{ cm}^{-3}$ and 10^{14} cm^{-3} diodes, respectively. The peak load voltages were 2.68 kV and 2.47 kV, respectively, Fig. 1(b). The simulation results show that the voltage drop on the load due to the displacement current in the pre-pulse region, $R_{Load} C dV_d/dt$, was 0.76 kV and 0.94 kV for the $1.5 \times 10^{10} \text{ cm}^{-3}$ and 10^{14} cm^{-3} -doped diodes, respectively.

The electric field during the switching of the 10^{14} cm^{-3} and $1.5 \times 10^{10} \text{ cm}^{-3}$ diodes is shown in Figs. 2(a) and 2(b), respectively. Because of the high doping, the electric field for the 10^{14} cm^{-3} -doped diode has a propagation front, and it requires around 0.4 ns for the ionization of n layer, in agreement with Refs. 6 and 24. The electric field for the $1.5 \times 10^{10} \text{ cm}^{-3}$ -doped diode has a uniform shape through most of the structure already during around 0.2 ns, and the impact ionization occurs simultaneously across the depletion region, in agreement with the results presented in Ref. 8.

In order to demonstrate the uniform behavior over a wide structure, a 520 μm , 4 mm^2 , SAS diode with $n = 10^{11} \text{ cm}^{-3}$ was simulated. The static breakdown voltage was 7.20 kV. The input voltage was $V(t) = 0.5V_0[1 - \cos(2\pi t/T)]$ with an amplitude of $V_0 = 14 \text{ kV}$ and a period of $T = 2 \text{ ns}$. We note that $V(t)$ up to $t = 1 \text{ ns}$ resembles the shape of the input pulse obtained in the experimental section,

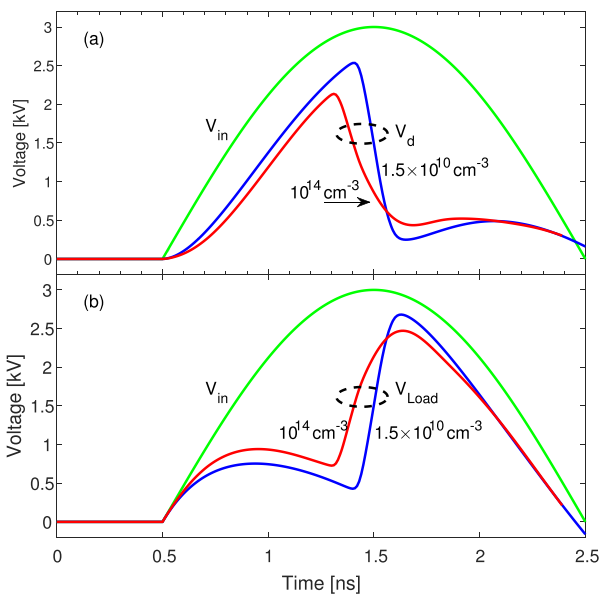


FIG. 1. Simulation of 100 μm thick, 4 mm^2 , SAS diodes with doping of 1.5×10^{10} and 10^{14} cm^{-3} . (a) The input voltage and the voltage on the diodes vs time. (b) The load voltage vs time.

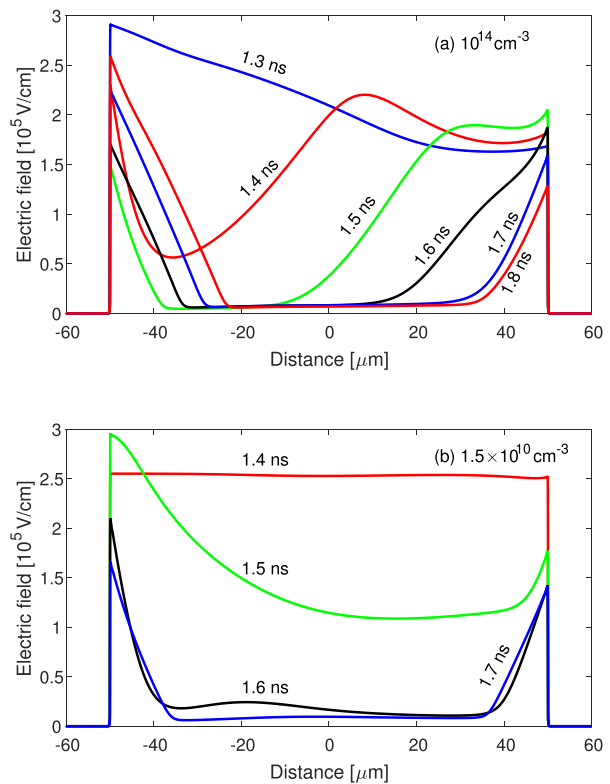


FIG. 2. Simulation of the electric field at various times during the switching in the 100 μm -thick SAS diodes with doping of 10^{14} cm^{-3} (a) and $1.5 \times 10^{10} \text{ cm}^{-3}$ (b).

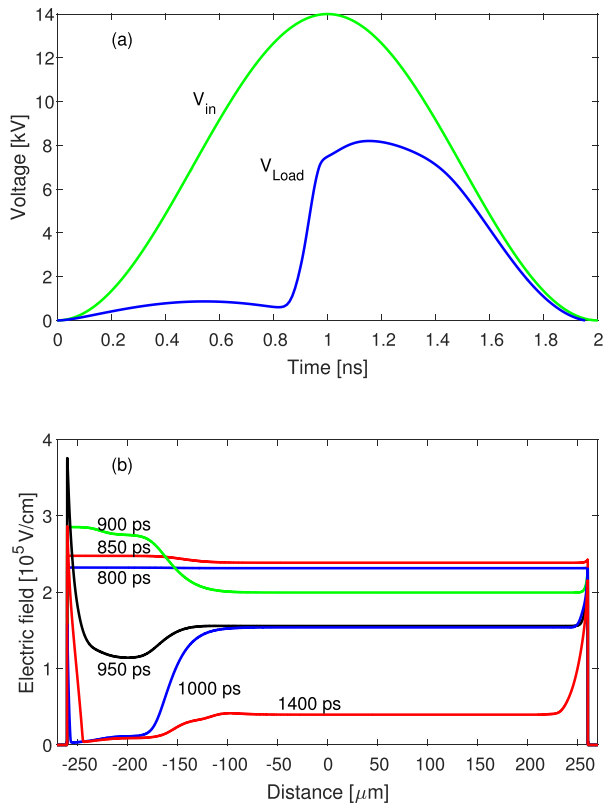


FIG. 3. Simulation of a 520 μm -thick, 4 mm^2 , SAS diode. (a) Input voltage and load voltage vs time. (b) The electric field profile during the switching time.

before the SAS is turned on (see below). The diode was connected in series between the input voltage source and the load, $R_{Load} = 50 \Omega$. Figure 3 shows the simulation results. As seen in Fig. 3(a), following a pre-pulse of 870 V, the load voltage rises to 7.3 kV within 100 ps. This rise time is comparable to the 100 μm SAS diode. The electric field, Fig. 3(b), is shown to have uniform behavior at time $t = 800$ ps, where the input voltage was 12.7 kV. The electric field is kept below 300 kV/cm until $t = 900$ ps, where the input voltage was 13.7 kV, and up to a maximum of 375 kV/cm near the anode at time $t = 950$ ps. The electric field at a time $t > 1000$ ps is uniform through most of the active region, keeping below 300 kV/cm near the device junctions.

A 517 μm SAS diode was fabricated using a float zone, 525 μm , n -type, (100), Si substrate with a resistivity of $10^4 \Omega \text{ cm}$. The p -type and n -type dopants were boron and phosphorous, with a diffusion

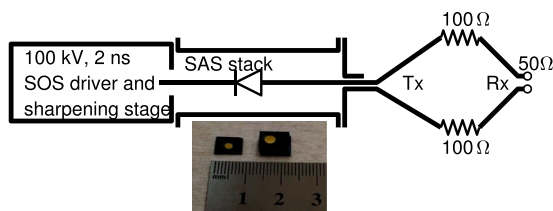


FIG. 4. Top: experimental setup (not to scale). Bottom: a photo showing a single 4 mm^2 diode and a stack of five 8 mm^2 diodes.

depth of about 4 μm for each dopant. The diode had a circular shape, defined by photolithography (see Fig. 4). It was cut from the wafer by cleaving so that the diode had a margin of ~ 2 mm.

The experimental setup is shown in Fig. 4. A solid-state generator based on magnetic-compression stages and two SOS stages³⁰ was used in this experiment to drive the SAS diode. To decrease the rise time of the driving voltage pulse, a stack of 16 DBDs was used at the output of the SOS generator. The generator produces pulses with a maximal amplitude up to 100 kV into a resistive 100 Ω load.

The generator output was fed into a 250 mm, transformer oil filled, coaxial transmission line (TL) having an impedance of around 50 Ω . A stack of five diodes with a junction cross section of 8 mm^2 was diced and connected in series, resulting in the total thickness of about 3 mm. Then, the stack was placed inside the TL at a distance of 150 mm from one end. The capacitance of this section was 15 pf.

In order to couple the power out from the TL, a 90 mm high-voltage coaxial cable, RG219/U, was connected at the other end. The other side of the cable was connected into a distributed losses network. The network consisted of a TEM horn transmitting antenna (“Tx”), a Vivaldi receiving antenna (“Rx”), and two 100 Ω high-voltage resistors, in which one was connected between the upper petal of the transmitting antenna and the upper petal of the receiving antenna and the other resistor between the lower petals of the transmitting and receiving antennas.

The network was characterized using a vector network analyzer by standard 50 Ω connectors, and its complex transmission coefficient at each frequency, S_{21} , was measured. The TL signal into the coaxial cable was obtained by measuring the network’s output temporal signal using an oscilloscope via a Barth high-voltage attenuator, transforming it into the frequency domain, dividing by S_{21} , and back into the time domain. The accuracy of this setup was determined to be ± 0.5 dB. It was benchmarked with a 6 kV/140 ps pulse and with a 5.5 kV/1 ns pulse by directly measuring these pulses using the Barth high-voltage attenuator and the oscilloscope.

Figure 5 shows the TL signal into the load, i.e., the 50 Ω coaxial cable followed by the distributed loss network and the high-voltage

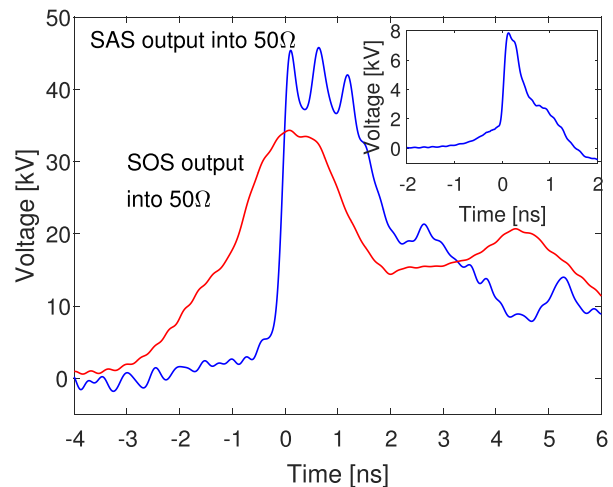


FIG. 5. Measurement of the stack of five 8 mm^2 diodes by the setup shown in Fig. 4. The inset shows the measurement of a single 4 mm^2 diode connected to a 50 Ω load, when driven by an ~ 14 kV pulse.

attenuator. When the SAS was placed inside the transmission line, the load voltage was 46 kV and its rise time (20%–90%) was 215 ps. The maximum voltage rise rate at the load was 192 kV/ns, and thus, the rise rate per diode can be estimated to be 38.4 kV/ns. The pre-pulse was 5.5 kV. Without the SAS, the generator output into the 50 Ω TL was 34 kV and its rise time (10%–90%) was 2.26 ns. We, therefore, estimate that the TL cavity between the SOS output and the SAS was charged up to about 100 kV by the SOS internal inductor, serving as a current source. The subsequent temporal compression ratio between the rise time of the driving pulse, 2.26 ns, and the SAS rise time, 215 ps, was 10.

In order to test a single diode, a diode with a junction cross section of 4 mm² was cleaved. A 5.5-kV, 1-ns pulsed power generator (measured on a 50 Ω load) was used to drive it. The generator output was connected via a 20 nH coil to a 1 pF peaking capacitor.^{9,31} The diode was connected in series between the capacitor and a 50 Ω load. The maximum voltage obtained at the peaking capacitor before the SAS turned on was about 14 kV. A peak load voltage of around 8 kV was obtained, Fig. 5(inset). Following a pre-pulse of about 1.5 kV, a sharp, 100 ps rise time was measured. The maximum voltage rise rate at the load was 57 kV/ns. These are the best updated results of rise rate and peak load voltage.

In conclusion, we showed that in order to obtain a high voltage SAS diode, with a rise time of the order of 100 ps, one can use a 525 μ m thick low-doped, $<10^{12}$ cm⁻³, substrate. In addition, we fabricated a stack of five diodes connected in series. The state-of-the-art performances of maximum output voltage and rise rate per diode of 8 kV and 57 kV/ns were demonstrated, respectively. The single-diode results are in good agreement with the simulation, Fig. 3(a), with the difference in the signal falling back to zero being dominated by the circuit, i.e., a peaking capacitor in the experiment vs a voltage source in the simulation.

To conclude, we enumerate several advantages of this diode. (a) The manufacturing of such devices becomes substantially easier since it is easy to handle thick wafers without the risk of breaking, and there is no need for deep, tens of micrometers, diffusion in order to narrow the active region. (b) The diode's structure allows the use of a small number of diodes in a stack in order to get to the tens of kilovolt operation range. (c) The stack's short length allows it to operate as a lumped element, with reduced parasitic inductance. (d) The lumped element operation of the five diodes results in stack overall capacitance reduced by a factor of five, hence lowering of the pre-pulse compared to the total pulse.

DATA AVAILABILITY

The data that support the findings of this study are available from the corresponding author upon reasonable request.

REFERENCES

- S. Rukin, "Pulsed power technology based on semiconductor opening switches: A review," *Rev. Sci. Instrum.* **91**, 011501 (2020).
- I. V. Grekhov and G. A. Mesyats, "Physical basis for high-power semiconductor nanosecond opening switches," *IEEE Trans. Plasma Sci.* **28**, 1540–1544 (2000).
- I. V. Grekhov, "Pulse power generation in nano- and subnanosecond range by means of ionizing fronts in semiconductors: The state of the art and future prospects," *IEEE Trans. Plasma Sci.* **38**, 1118–1123 (2010).
- J. Mankowski and M. Kristiansen, "A review of short pulse generator technology," *IEEE Trans. Plasma Sci.* **28**, 102–108 (2000).
- P. Rodin, U. Ebert, W. Hundsdorfer, and I. Grekhov, "Tunneling-assisted impact ionization fronts in semiconductors," *J. Appl. Phys.* **92**, 958–964 (2002).
- P. Rodin, U. Ebert, W. Hundsdorfer, and I. V. Grekhov, "Superfast fronts of impact ionization in initially unbiased layered semiconductor structures," *J. Appl. Phys.* **92**, 1971–1980 (2002).
- P. Rodin, P. Ivanov, and I. Grekhov, "Performance evaluation of picosecond high-voltage power switches based on propagation of superfast impact ionization fronts in SiC structures," *J. Appl. Phys.* **99**, 044503 (2006).
- P. Rodin and M. Ivanov, "Spatiotemporal modes of fast avalanche switching of high-voltage layered semiconductor structures: From subnano to picosecond range," *J. Appl. Phys.* **127**, 044504 (2020).
- A. S. Kesar, L. M. Merensky, M. Ogranovich, A. F. Kardo-Sysoev, and D. Shmilovitz, "6-kV, 130-ps rise-time pulsed-power circuit featuring cascaded compression by fast recovery and avalanche diodes," *Electron. Lett.* **49**, 1539–1540 (2013).
- L. M. Merensky, A. F. Kardo-Sysoev, D. Shmilovitz, and A. S. Kesar, "The driving conditions for obtaining subnanosecond high-voltage pulses from a silicon-avalanche-shaper diode," *IEEE Trans. Plasma Sci.* **42**, 4015–4019 (2014).
- A. S. Kesar, Y. Sharabani, L. M. Merensky, I. Shafir, and A. Sher, "Drift-step-recovery diode characterization by a bipolar pulsed power circuit," *IEEE Trans. Plasma Sci.* **40**, 3100–3104 (2012).
- A. S. Kesar, Y. Sharabani, I. Shafir, S. Zoran, and A. Sher, "Characterization of a drift-step-recovery diode based on all epi-Si growth," *IEEE Trans. Plasma Sci.* **44**, 2424–2428 (2016).
- A. S. Kesar, "A compact, 10-kV, 2-ns risetime pulsed-power circuit based on off-the-shelf components," *IEEE Trans. Plasma Sci.* **46**, 594–597 (2018).
- S. Yatomi, E. Stambulchik, V. Vekselman, and Y. E. Krasik, "Spectroscopic study of plasma evolution in runaway nanosecond atmospheric-pressure He discharges," *Phys. Rev. E* **88**, 013107 (2013).
- A. S. Kesar, "Underground anomaly detection by electromagnetic shock waves," *IEEE Trans. Antennas Propag.* **59**, 149–153 (2011).
- A. F. Kardo-Sysoev, "New power semiconductor devices for generation of nano- and subnanosecond pulses," in *Ultra-Wideband Radar Technology*, edited by J. D. Taylor (CRC Press, New York, 2001), Chap. 9.
- I. V. Grekhov, A. F. Kardo-Sysoev, L. S. Kostina, and S. V. Shenderoy, "High-power subnanosecond switch," *Electron. Lett.* **17**, 422–423 (1981).
- I. V. Grekhov, S. V. Korotkov, A. L. Stepaniants, D. V. Khristyuk, V. B. Voronkov, and Y. V. Aristov, "High-power semiconductor-based nano and subnanosecond pulse generator with a low delay time," *IEEE Trans. Plasma Sci.* **33**, 1240–1244 (2005).
- I. V. Grekhov, S. V. Korotkov, and P. B. Rodin, "Novel closing switches based on propagation of fast ionization fronts in semiconductors," *IEEE Trans. Plasma Sci.* **36**, 378–382 (2008).
- A. Gusev, M. Pedos, S. Rukin, S. Timoshenkov, and S. Tsyranov, "Semiconductor sharpeners providing a subnanosecond voltage rise time of GW-range pulses," *Rev. Sci. Instrum.* **88**, 114704 (2017).
- S. K. Lyubutin, S. N. Rukin, B. G. Slovikovsky, and S. N. Tsyranov, "High-power ultrafast current switching by a silicon sharpener operating at an electric field close to the threshold of the Zener breakdown," *IEEE Trans. Plasma Sci.* **38**, 2627–2632 (2010).
- A. F. Kardo-Sysoev and M. V. Popova, "Modeling of fast ionization waves in silicon pn junctions under breakdown," *Semiconductors* **30**, 431–435 (1996).
- V. Brylevskiy, I. Smirnova, A. Gutkin, P. Brunkov, P. Rodin, and I. Grekhov, "Delayed avalanche breakdown of high-voltage silicon diodes: Various structures exhibit different picosecond-range switching behavior," *J. Appl. Phys.* **122**, 185701 (2017).
- V. Brylevskiy, N. Podolska, I. Smirnova, P. Rodin, and I. Grekhov, "Picosecond-range avalanche switching initiated by a steep high-voltage pulse: Si bulk samples versus layered pn junction structures," *Phys. Status Solidi B* **256**, 1800520 (2019).
- A. Gusev, S. Lyubutin, S. Rukin, B. Slovikovsky, and S. Tsyranov, "On the picosecond switching of a high-density current (60 ka/cm²) via a Si closing switch based on a superfast ionization front," *Semiconductors* **48**, 1067–1078 (2014).
- Sentaurus Device User Guide* (Synopsys, Mountain View, CA, 2019).

²⁷*Compact Models User Guide* (Synposys, Mountain View, CA, 2019).

²⁸A. Chynoweth, "Ionization rates for electrons and holes in silicon," *Phys. Rev.* **109**, 1537 (1958).

²⁹J. Liou, "Modeling the tunnelling current in reverse-biased p/n junctions," *Solid State Electron.* **33**, 971–972 (1990).

³⁰S. Rukin, "High-power nanosecond pulse generators based on semiconductor opening switches," *Instrum. Exp. Tech.* **42**, 439–467 (1999).

³¹L. M. Merensky, A. F. Kardo-Sysoev, A. N. Flerov, A. Pokryvailo, D. Shmilovitz, and A. S. Kesar, "A low-jitter 1.8-kV 100-ps rise-time 50-kHz repetition-rate pulsed-power generator," *IEEE Trans. Plasma Sci.* **37**, 1855–1862 (2009).